

Supporting Information

Highly Oriented and Polyoxometalate-Incorporating Surface-Attached Metal-Organic Frameworks for Efficient Dye Adsorption and Water Oxidation

Xiu-Jun Yu,^{*a,b} Hai Zhong,^c Yi-Ming Xian,^a Ze-Ping Wang,^a Sebastian Schneider,^a Julian Scherr,^a Tarek Abu-Husein,^a Zhuo Zhang^{*d} and Andreas Terfort^{*e,a}

^aInstitute of Inorganic and Analytical Chemistry, University of Frankfurt, Frankfurt 60438, Germany

^bCenter for Self-assembly and Complexity, Institute for Basic Science, Pohang 37673, Republic of Korea

^cState Key Laboratory of Advanced Metallurgy, University of Science and Technology, Beijing 100083, China

^dSchool of Physics and Physical Engineering, Qufu Normal University, Qufu 273165, China

^eSchool of Cyber Science, Nankai University, Tianjin 300350, China

Contents

1. Experimental Details	S2
<i>1.1 Chemicals and Materials</i>	S2
<i>1.2 Preparation of Precursor Solutions</i>	S2
<i>1.3 SAM-Functionalized Substrates</i>	S2
<i>1.4 Spin-Coating and Alcohol Vapour Induced Growth</i>	S3
<i>1.5 Quantization of the Adsorption Capacities</i>	S3
<i>1.6 Dye Adsorption and Desorption Experiments</i>	S4
<i>1.7 Electrocatalytic Characterization and Measurements</i>	S4
<i>1.8 Microscopic and Spectroscopic Characterization</i>	S4
2. Supplementary Figures	S6
3. Tables	S14
4. References	S15

1. Experimental details

1.1 Chemicals and Materials: All the reagents except for vanadium-substituted phosphomolybdate (VPMo, $(n\text{-Bu}_4\text{N})_4\text{H}(\text{PMo}_{10}\text{V}_2\text{O}_{40})$, synthesized according to Ref. [1]) and the solvents employed were commercially available and used as supplied without further purification unless stated otherwise.

1.2 Preparation of Precursor Solutions: The preparation procedure of HKUST-1 precursor solution was the same as we published previously.^[2,3] Namely, 1.22 g of $\text{Cu}(\text{NO}_3)_2 \cdot 3\text{H}_2\text{O}$ (5.24 mmol) and 0.58 g of 1,3,5-benzenetricarboxylic acid (2.76 mmol) were dissolved in 5 g of dimethylsulfoxide (DMSO).

PTA@HKUST-1 and VPMo@HKUST-1 precursors were prepared in a similar way. 1.22 g of $\text{Cu}(\text{NO}_3)_2 \cdot 3\text{H}_2\text{O}$ (5.24 mmol), 0.58 g of 1,3,5-benzenetricarboxylic acid (2.76 mmol) and 1.0 g of phosphotungstic acid (PTA) or VPMo were dissolved in 5 g of DMSO.

The preparation of PMA@HKUST-1 precursor was slightly modified. 1.22 g of $\text{Cu}(\text{NO}_3)_2 \cdot 3\text{H}_2\text{O}$ (5.24 mmol) and 1.0 g of phosphomolybdic acid (PMA) were dissolved in 3 g of sulfolane to obtain solution A. At the same time, 0.58 g of 1,3,5-benzenetricarboxylic acid (2.76 mmol) was dissolved in 2 g of DMSO to get solution B. Finally, solution A was added into solution B under stirring to produce PMA@HKUST-1 precursor.

1.3 SAM-Functionalized Substrates: Au substrates were manufactured by electron-beam evaporation of 5 nm of Cr and 200 nm of Au onto four inch Si wafers with [100] orientation. After storage, these substrates were cleaned by immersion into a 10 mM 1-hexadecanethiol (HDT) solution in ethanol for 2 h followed by a 2 min treatment in H_2 plasma. The clean gold substrates were immersed for 48 h in a 0.1 mM of PPP1 ((4-(4-(4-pyridyl)phenyl)phenyl) methanethiol, synthesized according to Ref. [4]) solution. All substrates were washed with ethanol before spin coating.

1.4 Spin-Coating and Alcohol Vapour Induced Growth of POM@HKUST-1 SURMOFs: 150 μL of the precursor solution was spin-coated onto the PPP1 SAM-functionalized gold substrates (2 cm \times 2 cm) at 5000 rpm for 15 s (WS-650sz Lite, Laurell). For nucleation from alcohol vapour, the substrate was quickly transferred into a desiccator containing some methanol or ethanol in a glass beaker. Subsequently, the pressure was reduced to 30 mbar for a period of time by means of a membrane pump. Finally, the gold substrate was washed with methanol or ethanol and dried with N_2 . To grow thicker POM@HKUST-1 SURMOFs, either of these cycles was repeated. The alcohols are suitable precipitating solvents to trigger the nucleation and growth of POM@HKUST-1 SURMOFs and the monodentate nature of PPP1 SAM allows the coordination to the Cu_2 paddle-wheel units in the axial position, which can further facilitate the oriented growth. Therefore, with the help of alcohol-vapour treatment and surface functionalized PPP1 SAM, oriented nucleation and growth of POM@HKUST-1 SURMOFs could be achieved. The utilized PPP1 SAM on gold substrate can also improve the adhesion and presumably the homogeneity of SURMOF growth.

1.5 Quantization of the Adsorption Capacities of Highly Oriented PTA@HKUST-1 SURMOF: Adsorption capacities of PTA@HKUST-1 SURMOF towards benzene were performed on QCM25 crystal oscillators (SRS, AT cut, 5 MHz) using a QCM200 controller (SRS). In order to grow PTA@HKUST-1 SURMOF on QCM electrode, the electrode was washed by ethanol and cleaned by H_2 plasma followed by immersion into a 0.1 mM solution of PPP1 in ethanol for 48 h. Afterwards, PTA@HKUST-1 SURMOF was deposited after ten combined cycles of spin-coating and alcohol-vapour induced growth. The mass of the SURMOF on the electrode was calculated by measuring the change of oscillation frequency of the crystal (Δf) before and after the deposition process according to the Sauerbrey equation.^[5]

For the measurement of adsorption capacity, the QCM device was mounted into a desiccator. To remove the accommodated guest molecules from the pores, the desiccator was purged with dry N_2 which led to a dramatic increase of frequency.

After several minutes, the frequency curve reached a plateau and the stable baseline was obtained. Subsequently, the analyte was led into the chamber and gas adsorption was observed by the frequency change. Finally, dry N₂ was purged into the desiccator again to remove the analyte.

1.6 Dye Adsorption and Desorption Experiments: Dye adsorption experiments were performed as follows: freshly deposited SURMOFs were put into 10 ml flasks and then evacuated at room temperature for 30 min. Subsequently, the samples were immersed in ethanolic solutions of dyes (the concentrations were 4 mg/L) at room temperature. At a given time, the concentrations of dye solutions were determined by measuring the absorbance using an UV-vis spectrophotometer. After an immersion time of 12 h the samples were removed from the solutions, rinsed with ethanol, and finally dried in a flux of nitrogen gas. In the case of dye desorption, dye loaded PTA@HKUST-1 SURMOFs were soaked into 25 mM NH₄Cl ethanol-water solution (the volume ratio of ethanol/water was 160) for different times.

1.7 Electrocatalytic Characterization and Measurements: All of the electrochemical measurements were carried out using a CHI660E electrochemical workstation in a three electrode system. As-grown samples, Pt wafer and saturated calomel electrode were used as the working, counter and reference electrodes, respectively. The iR correction was applied to all data. The experimental potentials were converted to RHE with the equation $E_{(RHE)} = E_{(calomel)} + (0.118 + 0.0591 \times \text{pH}) \text{ V}$. Linear sweep voltammetry (LSV) and cyclic voltammetry (CV) measurements were performed at room temperature in an electrolyte of 80 mM B(OH)₃ with pH = 8 (adjusted using 1 M NaOH).

1.8 Microscopic and Spectroscopic Characterization: Surface X-ray diffraction (SXRD) measurements were performed in theta/theta mode, with a step width of 0.02°, and a scan rate of 100s/step. Infrared reflection-absorption (IRRA) spectra were recorded with a NICOLET 6700 Fourier transform infrared reflection-absorption spectrometer. For the SURMOFs a modified smart SAGA unit providing an incidence

angle of 80° was utilized. SAMs of perdeuterated hexadecanethiol ($C_{16}D_{33}SH$) on gold were used as background samples for the thin film FT-IR measurement. UV-vis spectra were collected using a Varian Cary 50 Scan UV-vis spectrophotometer. SEM images were recorded on a JEOL JSM 7001F scanning electron microscope at an acceleration voltage of 15 kV. The samples were sputtered with gold for 40 s using Edwards S150B sputter coater before SEM observation.

2. Supplementary Figures

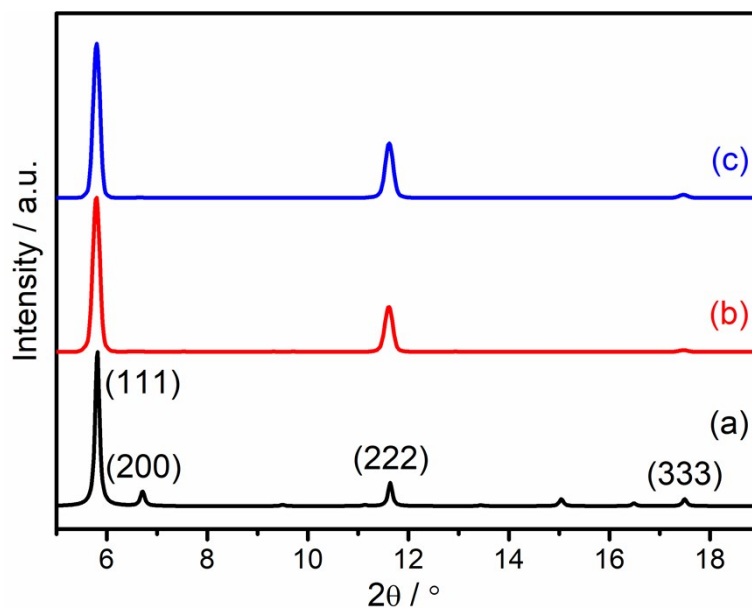


Figure S1 Out-of-plane XRD patterns of PTA@HKUST-1 SURMOF grown on PPP1 surface at RT after ten combined cycles of spin-coating and alcohol-vapour induced growth. (a) Simulated pattern; (b) methanol vapour treatment; and (c) ethanol vapour treatment.

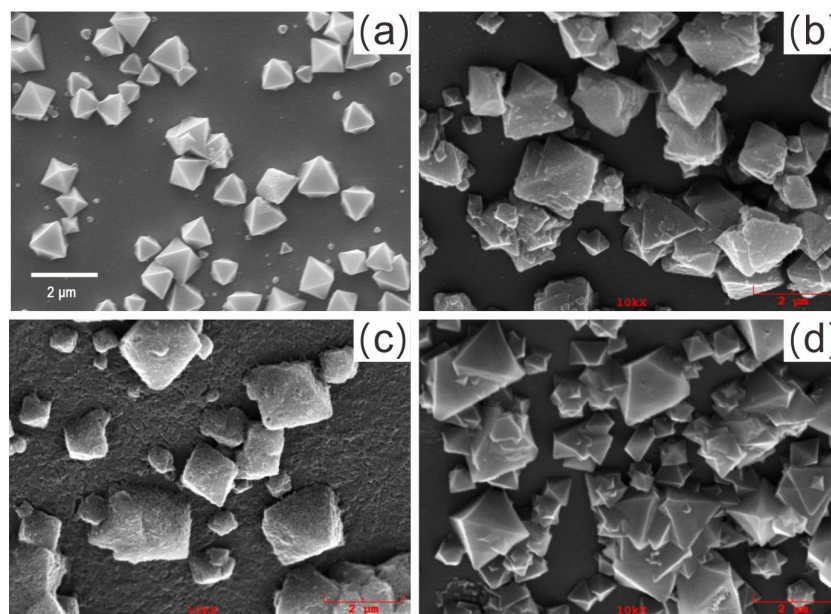


Figure S2 SEM images of PTA@HKUST-1 SURMOF grown on PPP1 surface at RT after one combined cycle of spin-coating and alcohol-vapour induced growth. (a) Methanol vapour for 15 min; (b) methanol vapour for 30 min; (c) methanol vapour for 45 min; and (d) ethanol vapour for 15 min.

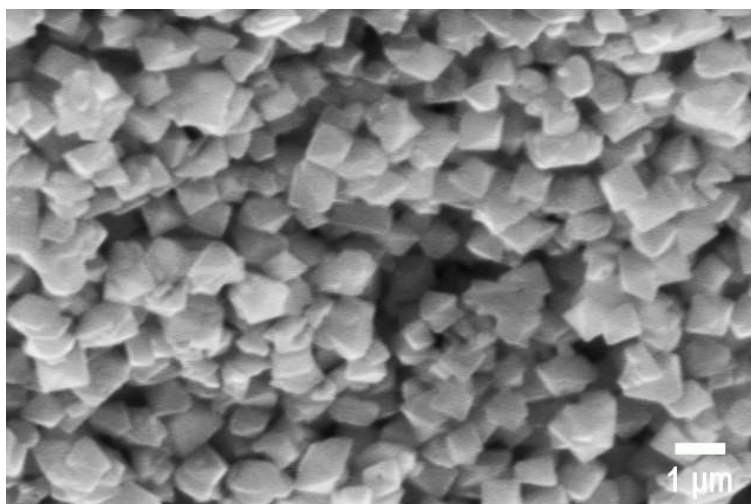


Figure S3 SEM image of PTA@HKUST-1 SURMOF grown on PPP1 surface at RT after ten combined cycles of spin-coating and methanol-vapour induced growth (15 min treatment for each cycle).

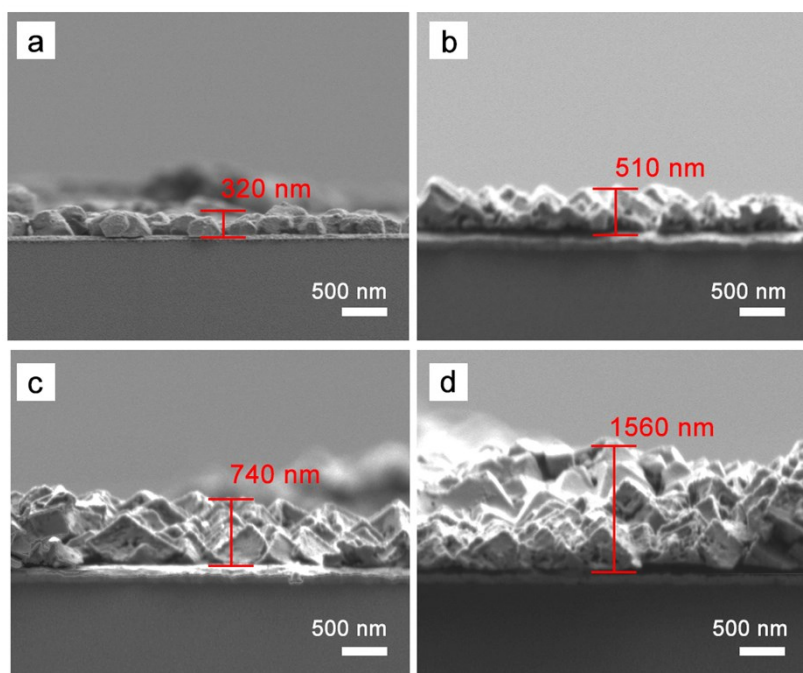


Figure S4 Cross-section SEM image of PTA@HKUST-1 SURMOF grown on PPP1 surface at RT after different combined cycles of spin-coating and methanol-vapour induced growth (15 min treatment for each cycle); (a) 3 cycles; (b) 5 cycles; (c) 7 cycles; and (d) 15 cycles. Each spin-coating cycle could increase the film thickness about 100 nm.

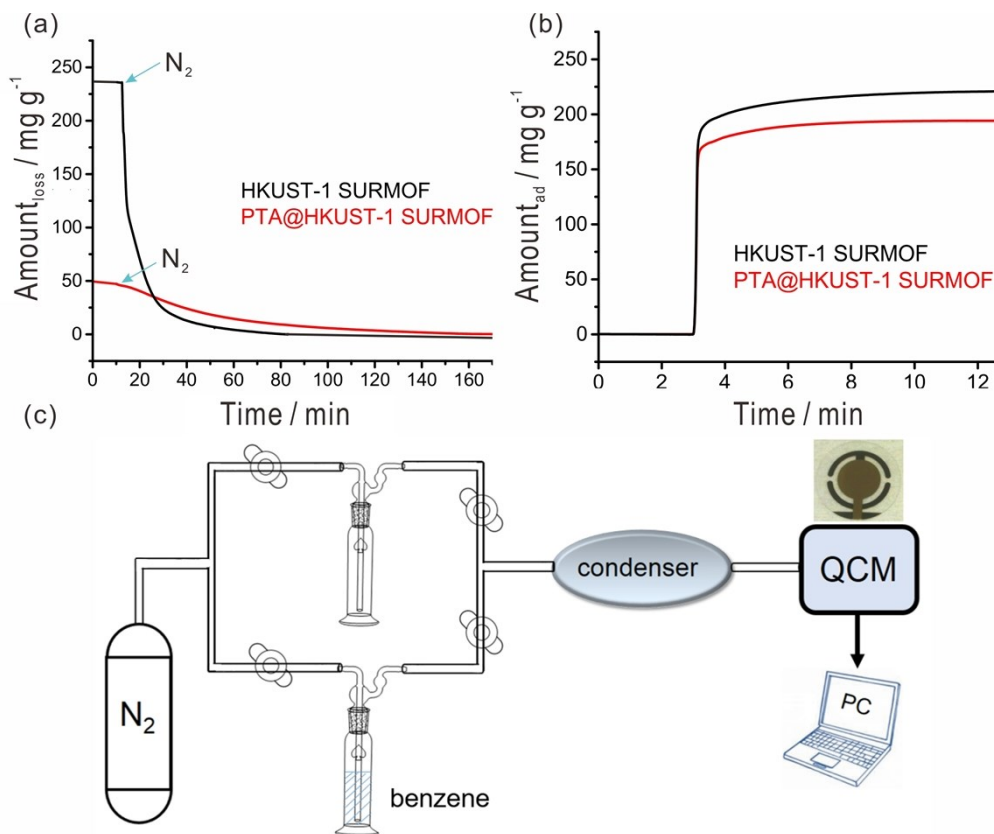


Figure S5 (a) Weight loss of HKUST-1 (black) and PTA@HKUST-1 (red) SURMOFs upon N₂ purge; (b) Adsorption capacities of HKUST-1 (black) and PTA@HKUST-1 (red) SURMOFs towards benzene; (c) Scheme of QCM adsorption setup.

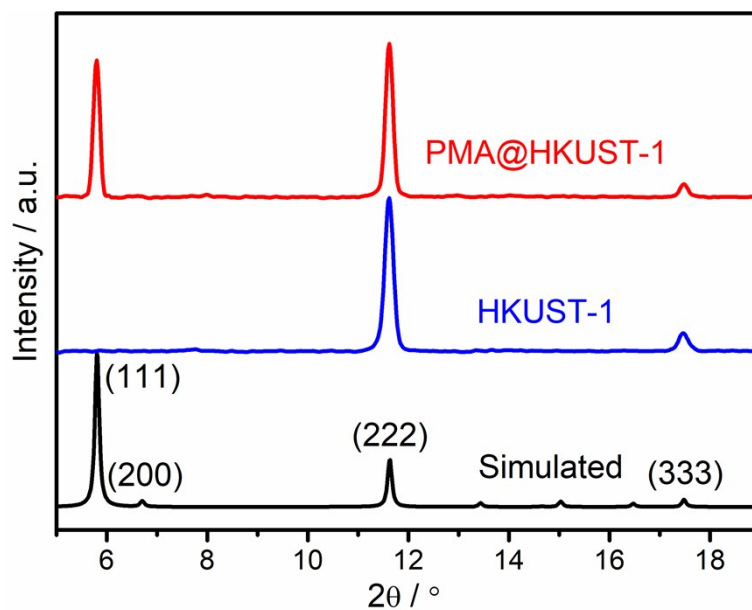


Figure S6 Out-of-plane XRD patterns of PMA@HKUST-1 and HKUST-1 SURMOFs fabricated by spin-coating (10 cycles) and methanol-vapour induced

growth (15 min treatment for each cycle) at RT on PPP1 surfaces.

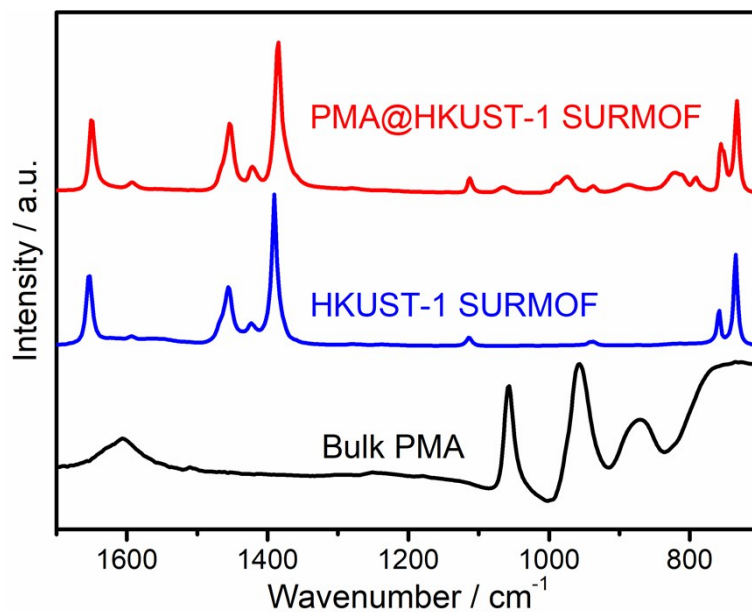


Figure S7 IRRA spectra of PMA@HKUST-1 and HKUST-1 SURMOFs fabricated by spin-coating (10 cycles) and methanol-vapour induced growth (15 min treatment for each cycle) at RT on PPP1 surfaces.

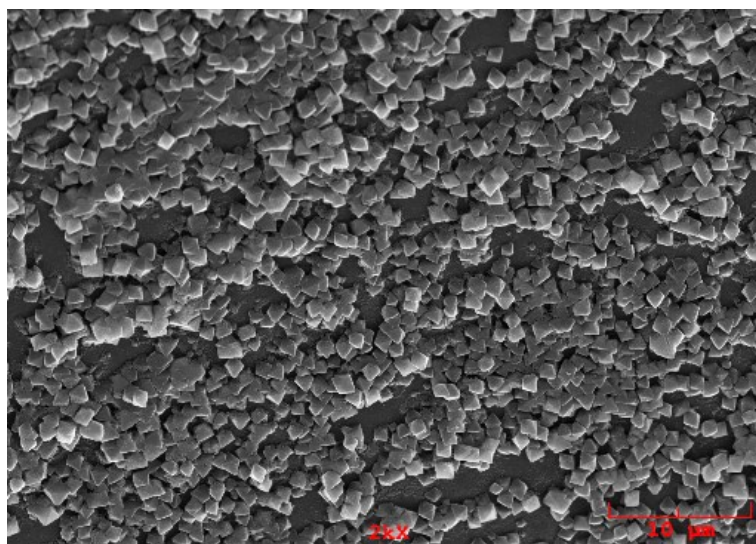


Figure S8 SEM image of PMA@HKUST-1 SURMOF grown on PPP1 surface at RT after three combined cycles of spin-coating and methanol-vapour induced growth (15 min treatment for each cycle).

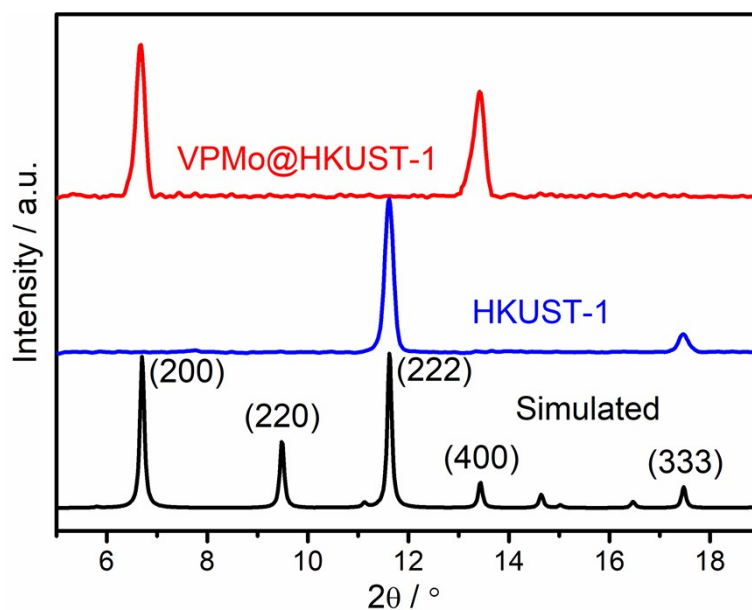


Figure S9 Out-of-plane XRD patterns of VPMo@HKUST-1 and HKUST-1 SURMOFs fabricated by spin-coating (10 cycles) and methanol-vapour induced growth (15 min treatment for each cycle) at RT on PPP1 surfaces.

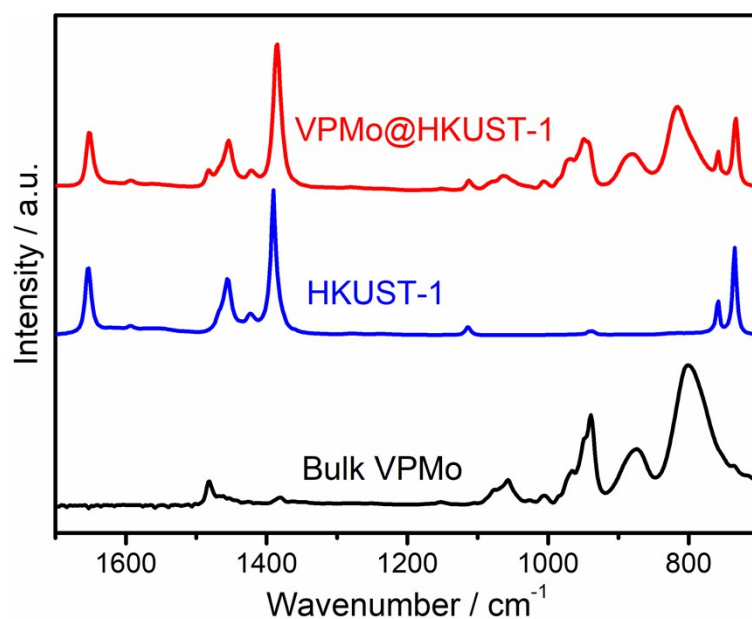


Figure S10 IRRA spectra of VPMo@HKUST-1 and HKUST-1 SURMOFs fabricated by spin-coating (10 cycles) and methanol-vapour induced growth (15 min treatment for each cycle) at RT on PPP1 surfaces.

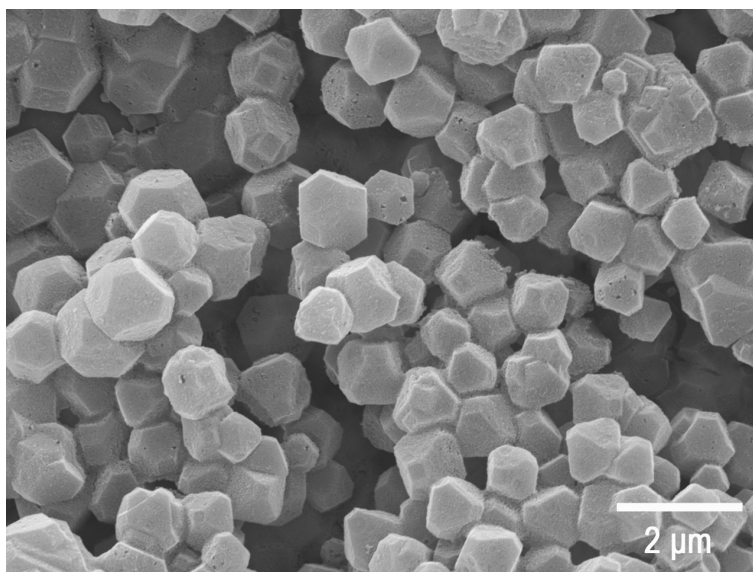


Figure S11 SEM image of VPMo@HKUST-1 SURMOF grown on PPP1 surface at RT after ten combined cycles of spin-coating and methanol-vapour induced growth (15 min treatment for each cycle).

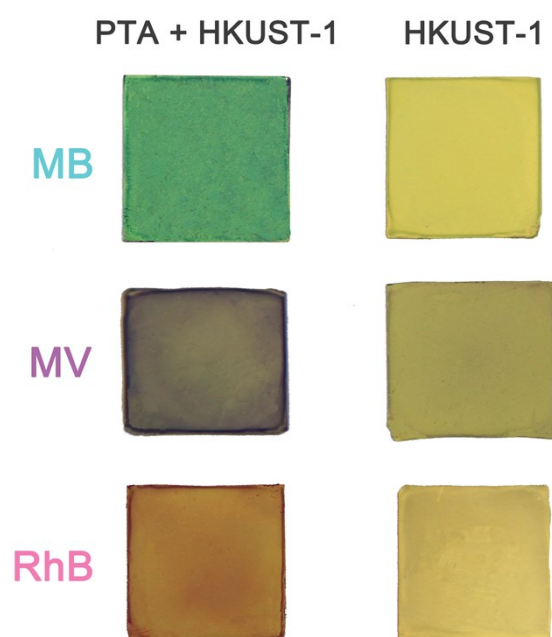


Figure S12 Colours of PTA@HKUST-1 and HKUST-1 SURMOFs after being immersed in the MB, MV and RhB ethanol solutions (the concentrations are 4 mg/L), demonstrating that the PTA@HKUST-1 SURMOF can serve as an efficient platform for the adsorption of cationic dyes.



Figure S13 Colours of PTA@HKUST-1 SURMOF (bottom) after being immersed in the dye mixtures and colours of 25 mM NH_4Cl ethanol-water solutions (top, the volume ratio of ethanol/water is 160) after soaking of the dye loaded PTA@HKUST-1 SURMOF, indicating the selective adsorption feature of PTA@HKUST-1 SURMOF.

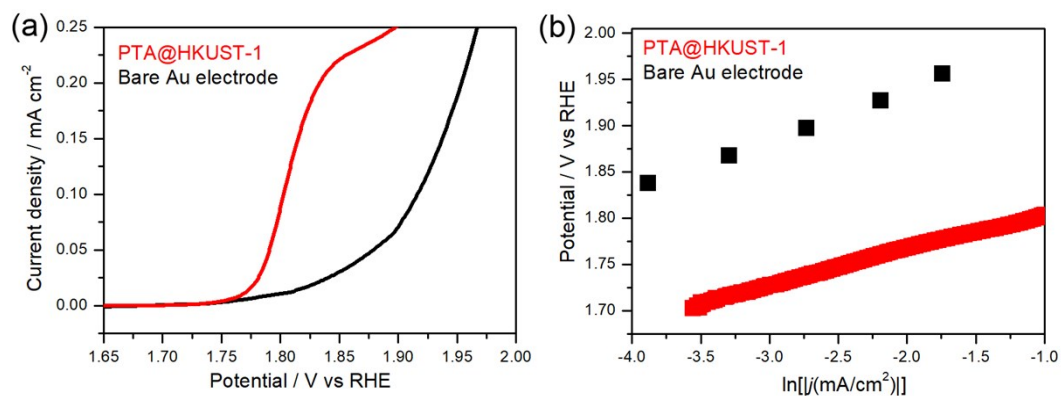


Figure S14 (a) OER-LSV curves of bare Au electrode (black) and PTA@HKUST-1 SURMOF (red) with the scan rate of 5 mV s^{-1} ; (b) Corresponding Tafel plots obtained from OER-LSV curves.

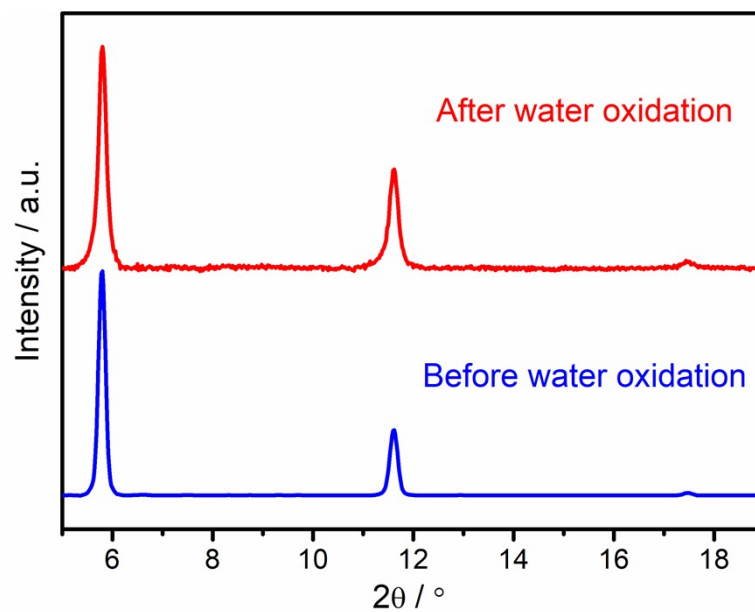


Figure S15 Out-of-plane XRD patterns of PTA@HKUST-1 SURMOFs before (blue) and after (red) water oxidation experiments, indicating that the SURMOF is robust enough in the OER process.

3. Tables

Table S1 Film thicknesses of PTA@HKUST-1 SURMOFs after different spin-coating cycles obtained based on cross-section SEM images shown in Figure S4.

Spin-coating cycles	Film thickness
3	320 nm
5	510 nm
7	740 nm
15	1560 nm

Table S2 Trace element analyses of PTA@HKUST-1 SURMOFs (two samples were deposited under the same conditions) based on TXRF measurements.

Element	Line	Concentration-1 / %	Concentration-2 / %
Cu	K12	41.474	41.480
W	L1	47.133	47.140
Au	L1	11.332	11.334

4. References

- [1] S. Himeno and N. Ishio, *J. Electroanal. Chem.*, 1998, **451**, 203–209.
- [2] J. L. Zhuang, D. Ceglarek, S. Pethuraj, and A. Terfort, *Adv. Funct. Mater.*, 2011, **21**, 1442–1447.
- [3] J. L. Zhuang, D. Ar, X. J. Yu, J. X. Liu, and A. Terfort, *Adv. Mater.*, 2013, **25**, 4631–4635.
- [4] B. Schüpbach and A. Terfort, *Org. Biomol. Chem.*, 2010, **8**, 3552–3562.
- [5] G. Sauerbrey, *Z. Phys.*, 1959, **155**, 206–222.